SCIENCE CHINA
Technological Sciences

Special Topic: High Entropy Alloys
• Review •

February 2018 Vol.61 No.2: 159–167
https://doi.org/10.1007/s11431-017-9051-6

Exploring the design of eutectic or near-eutectic multicomponent alloys: From binary to high entropy alloys

DING ZhaoYi, HE QuanFeng & YANG Yong*

Centre for Advanced Structural Materials, Department of Mechanical and Biomedical Engineering, City University of Hong Kong, Hong Kong SAR, China

Received January 18, 2017; accepted April 10, 2017; published online May 23, 2017

Eutectic and near-eutectic high entropy alloys (HEAs) have recently attracted a great deal of interest because of their promising properties, such as an excellent castability and unique combination of good ductility and high strength. However, in the absence of a phase diagram, it remains a non-trivial task to find a eutectic or near-eutectic composition for a HEA system, which usually demands a tremendous amount of efforts if a trial-and-error approach is followed. In this paper, we briefly review the thermodynamics that governs the eutectic solidification in regular binary and ternary alloys, and proceed to the discussion for the design of eutectic HEAs. Based on the data reported, we then propose an improved strategy which may enable an efficient search for the eutectic or near eutectic HEA compositions.

high entropy alloys, eutectic composition, phase stability, alloy design

Citation: Ding Z Y, He Q F, Yang Y. Exploring the design of eutectic or near-eutectic multicomponent alloys: From binary to high entropy alloys. Sci China Tech Sci, 2018, 61: 159–167, https://doi.org/10.1007/s11431-017-9051-6

1 Introduction

As originating from the Greek language, eutectics, a compound word of "eu"(-easy) and "teksis"(-melting), describes a non-unary system with a specific atomic or molecular ratio which has the lowest melting point. Upon solidification of eutectic alloys, competitive nucleation [1] and cooperative growth [2] of at least two phases are usually involved. Depending on the cooling rate and undercooling, eutectic or near eutectic alloys are able to yield different kinds of microstructures [3,4]. Typical microstructures of eutectic alloys include lamellar or rod-like [5–8] structures, which could lead to excellent mechanical properties for engineering applications. For example, eutectic Sn-Ag/Cu [9] with good mechanical properties, wettability was developed as reliable solder materials in absence of Pb element.

Recently, high entropy alloys (HEAs) were developed as equal or near equal atomic multicomponent alloys [10]. Unlike the conventional alloy design strategy which is usually based one major element, HEAs are defined as an alloy with five or more principal elements. As a new class of potential structural material, HEAs exhibit good mechanical properties. For example, $Al_{0.3}CoCrFeNi$ [11,12] displayed over 40% tensile elongation till failure both under the as-cast and annealing conditions. Meanwhile, $Al_{0.4}Hf_{0.6}NbTaTiZr$, $AlMo_{0.5}NbTa_{0.5}TiZr$ [13] and $Al_{0.5}NbTa_{0.8}Ti_{1.5}V_{0.2}Zr$ [14] attain a high yield strength even at a temperature over 800°C. High hardness values were also obtained when an appropriate alloying element was included in the CoCrFeMnNiV [15] and $AlCo_xCrFeMo_{0.5}$ [16] systems. In theory, due to the high entropy effect at equal or near-equal atomic ratios [10], the multicomponent systems tend to form single phase structures. However, it is known that a single-phased structure may not lead to a good combination of strength and plasticity

*Corresponding author (email: yonyang@cityu.edu.hk)

[17–19]. Therefore, a rather novel concept called "eutectics high entropy alloys" (EHEAs) were recently proposed [20–30]. By having two or even more competitive phases, such as an entropy stabilized solid solution phase and an intermetallic phase, EHEAs can possess the excellent balance of high ductility and strength [20]. Besides, because of the sluggish diffusion at elevated temperature [31], EHEAs may have the potential to be used as high-temperature alloys. For example, the $AlCoCrFeNi_{2.1}$ [20,25,32] EHEA system possessing the FCC/B2 phases exhibits a tensile fracture stress of 944 MPa and failure strain of 25.6% at room temperature, 538 MPa and 22.9% at 973 K, 690 MPa and 6.7% at 77 K. The $AlCrFeNiMo_{0.5}$ EHEA [33] with the mixture of two BCC phases reaches a very high fracture stress at 2643.5 MPa with a fracture strain comparable to that of a low carbon stainless steel [34]. The CoCrFeNiNbx EHEA [24,29] displayed a high hardness around 700 HV or 7 GPa in the as cast state and retained a residual strength as high as 3 GPa even after 24 h of thermal annealing at 1023 K.

Despite the promising properties of EHEAs, it is not a trivial task to locate eutectic compositions, if any, for a given HEA system due to the lack of a phase diagram. In the literature, the concept of a pseudo binary-phase EHEA [23,35,36] was often mentioned, which was based on the notion that an EHEA system may comprise of two phases similar to a regular binary alloy, with one phase to be entropy stabilized at a high temperature. With the database-based computational packages, such as Thermo-Calc, one can even attempt to verify the eutectic composition if the so-called pseudo-phase EHEA system was already identified. Trial-and-error methods [22,23,26] were also conducted for the verification of the eutectic composition for HEAs. Usually, this was done by checking whether one could observe a hypo- or hyper- like eutectic microstructures to fine tune the alloy compositions. In principle, this process is time consuming and empirical in nature. In this article, we propose a systematic approach to design EHEAs after a brief reviewing of the fundamental thermodynamics governing the formation of eutectic composition. This approach is later justified with the EHEA compositions reported so far.

2 Eutectic binaries and ternaries

2.1 Thermodynamics of eutectic formation in multi-component alloys

Upon the solidification of a eutectic alloy system, multiple phases precipitate at the same time. In theory, the eutectic composition and eutectic temperature might be predicted with Schroeder-van Laar equation [37] should all the eutectic phases precipitated are known a priori. In general, it can be easily shown that the following relation between the Gibb's free energy G, temperature T and enthalpy H holds at a constant pressure P. According to ref. [38], it can be easily shown that

$$\left.\frac{\partial(G/T)}{\partial T}\right|_P = -\frac{H}{T^2}, \tag{1}$$

Note that the expression of entropy $S = -\partial G/\partial T|_P$ and Gibb's free energy $G = H - TS$ are used in deriving eq. (1). Upon the mixing of different phases, the chemical potential of the ith phase can be expressed as $\mu_i = \mu_i^0 + RT\ln(a_i/a)$ where μ_i^0 is the chemical potential of ith phase before mixing, R is the gas constant, a_i is the activity coefficient of the ith phase and a is the reference activity coefficient. Given the general relationship $G = \sum_{i=1}^{n}\mu_i X_i$ where X_i is the molar fraction of the ith phase, one could obtain the following equation for solidification of the ith phase:

$$\left.\frac{\partial(\mu_i/T)}{\partial T}\right|_P = -\frac{\Delta H^i_{\text{fusion}}}{T^2}, \tag{2}$$

where $\Delta H^i_{\text{fusion}}$ is the enthalpy of fusion of ith phase. Let us further assume an ideal mixing of the eutectic phases, we then have $\frac{\alpha_i}{\alpha} = X_i$. As such, eq. (2) can be cast into $\left.\frac{\partial(RlnX_i)}{\partial T}\right|_P = -\frac{\Delta H^i_{\text{fusion}}}{T^2}$. Integrating the above equation thereby gives the set of Schroeder-van Laar equations for a eutectic solidification [37]:

$$\ln X_i = \frac{\Delta H^i_{\text{fusion}}}{R}\left(\frac{1}{T_E} - \frac{1}{T_i}\right). \tag{3}$$

In which i goes from 1 to n, $\sum_{i=1}^{n} X_i = 1$; T_E is the eutectic temperature of the alloy and T_i is the melting point of phase i. Note that the boundary condition $T=T_i$ for $X_i=100\%$ is used in deriving eq. (3).

2.2 Regular binary and ternary alloys

First, let us verify the applicability of eq. (3) on binary eutectics. For the sake of simplicity, we herein focus on the binary solid-solution eutectic alloys. As such, the enthalpy of fusion and melting temperature of the individual element, as listed in Table 1, can be used as the inputs to eq. (3). As shown in Figure 1(a) and (b), it can be seen that eq. (3) captures very well the general trend of the eutectic temperature T_E and eutectic composition obtained across a wide range of alloy systems. The data scattering may be attributed to the assumption of ideal mixing.

Next, we verify the predictability of eq. (3) on eutectic ternary solid-solution systems. Although the theoretical prediction of the eutectic temperature generally agrees with the experimental data as shown in Figure 2(a), however, it can be noticed that a relatively large discrepancy arises between the predicted and measured eutectic compositions, as listed in

Table 1 The melting point (K), eutectic temperature (K), enthalpy of fusion (J mol^{-1}), calculated and experimentally measured for the binary systems. The experimental data of the eutectic temperature are from [39] while the data of the melting point and enthalpy of fusion are from [40][a)]

	Enthalpy of fusion (J mol^{-1})	Melting point (K)	Calculated molar fraction and eutectic temperature	Experiment molar fraction and eutectic temperature		Enthalpy of fusion (J mol^{-1})	Melting point (K)	Calculated molar fraction and eutectic temperature	Experiment molar fraction and eutectic temperature
Al	10700	934	0.05	0.05	Ge	31800	1211	0.23	0.16
Ga	5590	303	0.95	0.95	Sb	19700	904	0.77	0.84
			T_E=297 K	T_E=299 K				T_E=823 K	T_E=865 K
Al	10700	934	0.8	0.71	Ge	31800	1211	0.07	0.05
Ge	31800	1210	0.2	0.29	Zn	7350	693	0.93	0.95
			T_E=803 K	T_E=697 K				T_E=656 K	T_E=667 K
Al	10700	934	0.34	0.12	Hf	25500	2506	0.36	0.32
Zn	7350	693	0.66	0.88	Th	16000	2023	0.64	0.68
			T_E=523 K	T_E=654 K				T_E=1372 K	T_E=1723 K
As	27700	887	0.56	0.57	Hf	25500	2506	0.29	0.13
Au	12500	1337	0.44	0.43	Y	11400	1799	0.71	0.87
			T_E=769 K	T_E=909 K				T_E=1244 K	T_E=1698 K
Au	12500	1337	0.62	0.75	La	6200	1193	0.93	0.9998
Co	16200	1768	0.38	0.25	Ta	36000	3290	0.06	0.0002
			T_E=940 K	T_E=1269.5 K				T_E=1075 K	T_E=1138 K
Au	12500	1337	0.61	0.7	Lu	22000	1926	0.52	0.63
Ge	31800	1210	0.39	0.3	Zr	21000	2128	0.48	0.37
			T_E=931 K	T_E=634 K				T_E=1310 K	T_E=1673 K
Au	12500	1337	0.88	0.96	Mo	36000	2896	0.23	0.23
Mo	36000	2896	0.12	0.04	Pa	15000	1845	0.77	0.77
			T_E=1120 K	T_E=1327 K				T_E=1457 K	T_E=1740 K
Au	12500	1337	0.64	0.915	Pb	4770	601	0.86	0.83
Tm	16800	1818	0.36	0.085	Sb	19700	904	0.14	0.17
			T_E=953 K	T_E=1115 K				T_E=518 K	T_E=524.7 K
Cr	20500	2180	0.48	0.27	Sc	16000	1814	0.8	0.88
Lu	22000	1936	0.52	0.73	Ta	36000	3290	0.2	0.12
			T_E=1315 K	T_E=1523 K				T_E=1492 K	T_E=1792 K
Cr	20500	2180	0.41	0.34	Ta	36000	3290	0.15	0.001
Sc	16000	1814	0.59	0.66	Tb	10800	1629	0.85	0.999
			T_E=1215 K	T_E=1363 K				T_E=1351 K	T_E=1627 K
Cr	20500	2180	0.36	0.22	Tb	10800	1629	0.64	0.77
Y	11400	1799	0.64	0.78	Ti	18700	1941	0.36	0.23
			$T_{E=}$1140 K	$T_{E=}$1514 K				T_E=1038 K	T_E=1543 K
Cu	13100	1358	0.79	0.975	Tb	10800	1629	0.68	0.65
Ru	25700	2607	0.21	0.025	Zr	21000	2128	0.32	0.35
			T_E=1128 K	T_E=1332 K				T_E=1092 K	T_E=1523 K
Dy	11100	1685	0.66	0.57	Ti	18700	1941	0.46	0.27
Zr	21000	2128	0.34	0.43	Tm	16800	1818	0.54	0.73
			T_E=1110 K	T_E=1553 K				T_E=1166 K	T_E=1603 K
Ga	5590	303	0.84	0.95	Y	11400	1799	0.64	0.6
Zn	7350	693	0.16	0.05	Zr	21000	2128	0.35	0.4
			T_E=281 K	T_E=298 K				T_E=1139 K	T_E=1636 K

a) Note that T_E stands for the eutectic temperature

Table 2. This implies that the applicability of the ideal mixing rule should be limited as the compositional complexity of an alloy system increases. A similar finding for the limitation of the ideal mixing rule for multi-component systems was also discussed in HEA literature [42,43]. Interestingly, from Table 2, one may notice that the constituent elements of the ternary eutectics also form binary eutectics pairwise. As an example, Table 3 lists the breakdown of the eutectic Cd-Pb-Sn, Cd-Sn-Tl and Al-Ge-Zn ternaries into several eutectic binaries. Indeed, a similar idea was proposed early in the literature [44,45], however, there is no verification done yet for multicomponent systems, particularly for HEAs, to our best knowledge. Here, one may envision that, if the above findings are generally valid, a formula for a eutectic multicomponent system may be available. That is, one may view a eutectic multicomponent system as a combination of several eutectic binaries. For instance, we may reformulate the above eutectic ternaries as $Cd_{23}Pb_{20}Sn_{57} = (Cd_{28}Pb_{72})_{0.2}(Cd_{33}Sn_{67})_{0.6}$-

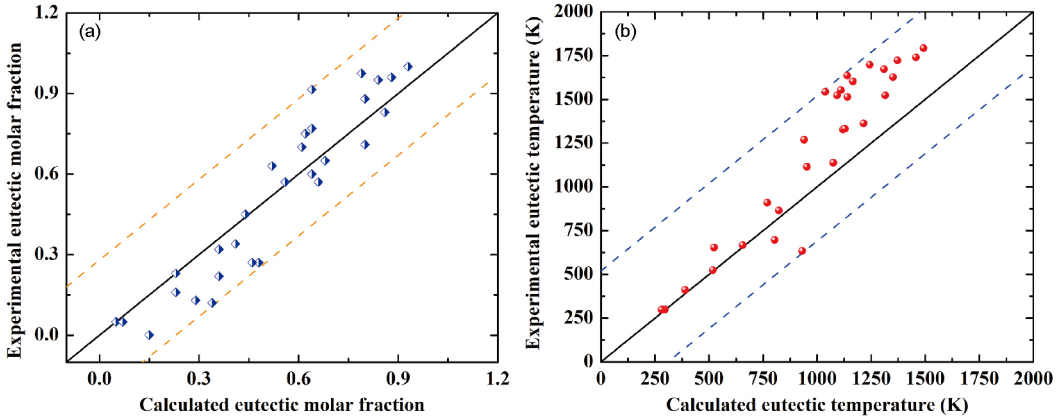

Figure 1 (Color online) Comparison of the calculated and measured (a) molar fraction of one constituent element and (b) the eutectic temperature for the eutectic binaries.

Table 2 The melting point (K), eutectic temperature (K), enthalpy of fusion (J mol^{-1}), calculated and experimentally measured for the selected ternary systems. The experimental data of the eutectic temperature are from [41] while the data of the melting point and enthalpy of fusion are from [40]. Note that the binary eutectic compositions are rounded to closest 1%

	Enthalpy of fusion (J mol^{-1})	Melting point (K)	Calculated molar fraction and eutectic temperature	Experiment molar fraction and eutectic temperature		Enthalpy of fusion (J mol^{-1})	Melting point (K)	Calculated molar fraction and eutectic temperature	Experiment molar fraction and eutectic temperature
Bi	10900	544	0.01	0.015	Ga	5590	303	0.68	0.859
Ga	5590	303	0.25	0.015	Sn	7000	505	0.2	0.074
Hg	2290	234	0.74	0.97	Zn	7350	693	0.12	0.067
			T_E=186 K	T_E=233 K				T_E=258 K	T_E=290 K
Al	10700	933	0.03	0.03	Cd	6300	594	0.27	0.22
Ga	5590	303	0.74	0.89	Sn	7000	505	0.3	0.51
Sn	7000	505	0.23	0.08	Tl	4200	577	0.43	0.27
			T_E=267 K	T_E=292 K				T_E=293 K	T_E=403 K
Cd	6300	594	0.29	0.23	Al	10700	933	0.33	0.15
Pb	4770	601	0.39	0.2	Ge	31800	1211	0.015	0.07
Sn	7000	505	0.32	0.57	Zn	7350	693	0.65	0.78
			T_E=301 K	T_E=418 K				T_E=519 K	T_E=~623 K

Table 3 The breakdown of the ternary eutectics into several eutectic binaries

Cd-Pb-Sn alloy			
Binary eutectic "elements"	$Cd_{28}Pb_{72}$	$Cd_{33}Sn_{67}$	$Pb_{26}Sn_{74}$
Cd-Sn-Tl alloy			
Binary eutectic "elements"	$Cd_{33}Sn_{67}$	$Cd_{27}Tl_{73}$	$Sn_{70}Tl_{30}$
Al-Ge-Zn alloy			
Binary eutectic "elements"	$Al_{70}Ge_{30}$	$Al_{12}Zn_{88}$	Ge_5Zn_{95}

$(Pb_{26}Sn_{74})_{0.2}$, $Cd_{22}Sn_{51}Tl_{27}=(Cd_{33}Sn_{67})_{0.5}(Cd_{27}Tl_{73})_{0.25}(Sn_{70}Tl_{30})_{0.25}$, and $Al_{15}Ge_7Zn_{78}=(Al_{70}Ge_{30})_{0.15}(Al_{12}Zn_{88})_{0.35}(Ge_5Zn_{95})_{0.5}$. In what follows, we will turn to HEAs and discuss further the above ideas about EHEAs.

3 High entropy alloys

3.1 Entropy stabilization and random solid solution

In 2004, Yeh et al. [10] proposed the concept of HEA to rationalize their findings of the formation of random solid solution in equal atomic multicomponent alloys. The idea of HEA was originally rooted in the ideal mixing rule, according to which the configurational entropy of mixing S_c per atom for a N-component random solid solution alloy may be expressed as $S_c = -k_B\sum_{i=1}^{N} X_i \ln X_i$. As such, the configurational entropy of mixing S_c reaches its theoretical maximum S_{id} in an equal atomic composition:

$$S_{id} = k_B \ln N, \tag{4}$$

where N is the total number of elements. As N increases from 3 to 6, S_{id} goes from 1.1 R to 1.79 k_B. According to Yeh et al. [10,46], this brings about a high entropy effect which could stabilize a random solid solution phase instead of intermetallics. However, the experiment results [47–49] reported so far simply showed that the formation of random solid solution depends not only on S_{id} but also on other parameters, such as the atomic size difference and mixing enthalpy of the constituent atomic pairs [50]. In analogy to the Hume-Rothery rules, Zhang et al. [51–53] further proposed several empirical parameters for the formation of random solid solution in HEAs. These include the atom size difference δ and the mixing enthalpy ΔH_{mix}, which can be expressed as $\delta\% = 100\%\sqrt{\sum_{i=1}^{n} X_i\left(1-\frac{r_i}{\sum_{j=1}^{n} X_j r_j}\right)^2}$, $\Delta H_{\mathrm{mix}} = \sum_{i=1,i\neq j}^{n} 4\Delta H_{ij}^{\mathrm{mix}} X_i X_j$, respectively where r_i is the atomic radius of the ith element and $\Delta H_{ij}^{\mathrm{mix}}$ is the enthalpy of mixing of binary alloys between the ith and jth elements. According to Zhang et al. [54], single phase HEAs tend to form for –15 kJ mol^{-1}<ΔH_{mix}<5 kJ mol^{-1} and 0<δ<5, and multiple phases and even amorphous structures tend to form otherwise.

In theory, eq. (4) holds if all interactions among the constituent elements in a HEA can be neglected. This may be plausible at a high temperature when thermal fluctuations outweigh all atomic-scale interactions. However, as the temperature cools below the melting point of an alloy, it may be imperative to consider the effect of atomic-scale interactions on the accessible microstates which an alloy can explore in its configurational space. Consequently, the configurational energy of mixing could reduce because of the variety of correlations resulting from the inter-atomic interactions. If one relaxes the assumption of an ideal mixing rule and takes the mixing of elements in a random solid solution to be correlated, the configurational entropy of mixing S_{corr} can be written as [55,56]:

$$S_{\mathrm{corr}} = S_{id} + S_E, \tag{5}$$

where S_E ($\leqslant$0) denotes the excess entropy of mixing. The physical meaning of S_E is that the variety of inter-atomic interactions could result in a reduction of configurational entropy of mixing and result in a deviation from ideal mixing rules. More specifically, S_E can be expressed as follows according to the recent work of He et al. [43]:

$$S_E = k_B \cdot \left[1 + \frac{x}{2} - \ln(x) + \ln(1-\mathrm{e}^{-x}) - \frac{x}{2}\cdot\frac{1+\mathrm{e}^{-x}}{1-\mathrm{e}^{-x}}\right], \tag{6}$$

where the dimensionless parameter $x = \frac{\Delta\varepsilon}{k_B T}$ stands for the normalized energy fluctuation due to atomic interactions and $\Delta\varepsilon$x is the range of interaction energies. In general, there are different kinds of inter atomic interactions which can contribute to the normalized energy fluctuation. According to He et al. [43], the energy fluctuation due to atomic size difference and chemical bond misfit can be respectively expressed as the two dimensionless parameters x_e and x_c. Consequently, one has x=x_e+x_c. Following refs. [43,47], it can be theoretically derived that:

$$x_e = 4.12\delta \cdot \sqrt{\frac{\overline{K}\,\overline{V}}{k_B T}}, \tag{7a}$$

$$x_c = 2\sqrt{\frac{\sqrt{\sum_i \sum_{j,i\neq j} X_i X_j (H_{ij}-\overline{H})^2}}{k_B T}}, \tag{7b}$$

where $\overline{K}$ is average bulk modulus, $\overline{V}$ is average atomic volume, H_{ij} is the mixing enthalpy between element i and j, and $\overline{H}$ is the average of H_{ij}. Based on the data reported in the literature, He et al. [43] found that the phase selection in HEAs is correlated very well with the ratio of S_{corr}/S_{id}. A single-phase solid solution tends to form for 0.85<S_{corr}/S_{id}<1; a multi-phase structure tends to appear for 0.7<S_{corr}/S_{id}<0.85; and an amorphous structure tends to form for 0.4<S_{corr}/S_{id}<0.6. This is consistent with the early finding of Zhang et al. [57]. As an example, Figure 2(b) shows the comparison of a few quinary HEAs of different phases. According to eq. (4), they share the same configurational entropy of mixing S_{id}=$k_B$ln5 as an ideal solution although they are of different phases in the as-cast state. In contrast, the alloys of different phases are well separated by their ratio of S_{corr}/S_{id}. These results are encouraging, which implies that the notion of entropy stabilization is valid, at least for the few single-phased HEAs.

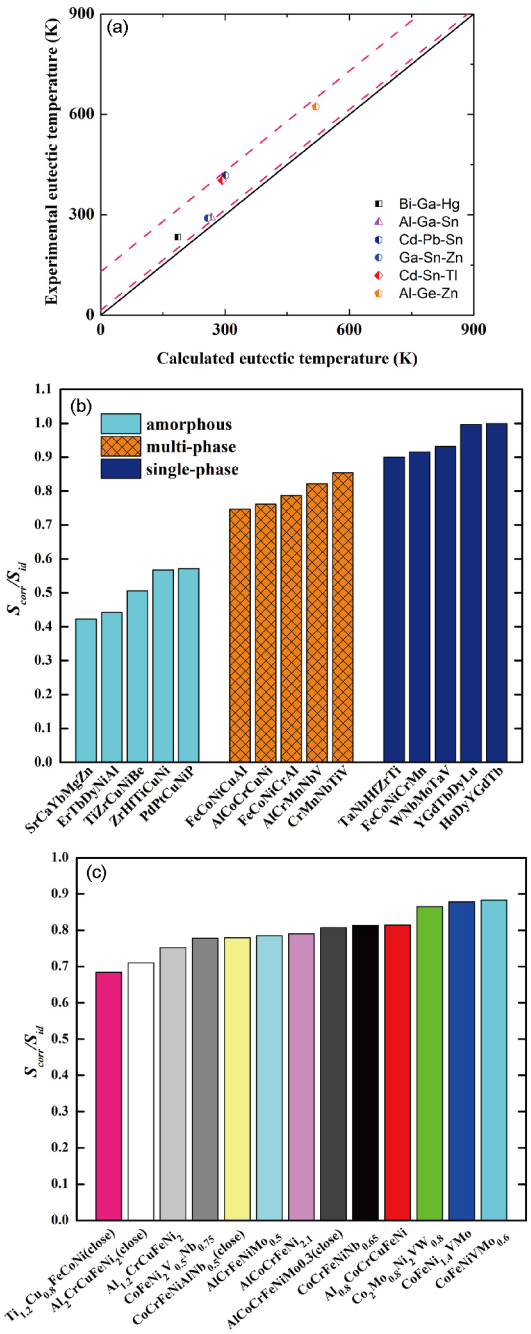

Figure 2 (Color online) (a) Comparison of ternary systems between calculated eutectic temperature and experimental temperature; (b) comparison of the S_{corr}/S_{id} ratios calculated for 15 quinary HEAs. Note that the average melting temperature according to the rule of mixture is used for the calculation of the correlated entropy S_{corr}; (c) comparison of the S_{corr}/S_{id} for reported eutectic or near eutectic compositions calculating at their melting temperature.

3.2 The effect of formation enthalpy

Alternatively, Troparevsky et al. [58] proposed a simple criterion based on the enthalpy of formation ΔH_f of all possible binaries to predict the phase formation in HEAs. Their idea was based on the notion that, for a given entropic contribution $-T_{ann}\Delta S_{mix}$, where T_{ann} is the annealing temperature and ΔS_{mix} is the ideal entropy of mixing, the strong (weak) interactions of pairwise constitutes promotes (suppresses) the multi-phase formation. In general, this is equivalent to the idea of entropic stabilization and the findings of Troparevsky et al. [58] are also consistent with those of Zhang et al. [57] since the enthalpy of formation ΔH_f is correlated with the enthalpy of mixing ΔH_{mix} for binaries [39].

4 Design of eutectic high entropy alloys

From thermodynamic view, the solidification behavior of a eutectic system is driven by Schroeder-van Laar equation. However, in high entropy alloys, the number of elements can reach as much as 7 which implies a large potential number of phases can co-precipitate when liquid metal solidifies. With absent of these phases information, we are not able to locate the eutectic point efficiently by conducting eq. (3). Moreover, none ideal mixing of metal atoms may induce a relative large deviation from where the eutectics should be.

Based on the above discussions, hypotheses can be now proposed for the formation of EHEAs, being listed as follows. Namely, (1) the mixing of the selected elements should lead to the formation of multiple phases by destabilizing the random solid solution single phase; however, amorphization should be discouraged since eutectic multicomponent systems could be potential metallic glass formers [59,60]; and (2) the multicomponent systems should contain eutectic binaries as the essential "elements" to form a eutectic multicomponent system. Here, it should be noted that satisfying (1) is equivalent to having $0.7<S_{corr}/S_{id}<0.85$ based on the prior data of HEAs [43].

Table 4 lists the EHEAs or near-eutectic HEAs hitherto reported in the HEA literature [20–24,26,28,36], from which it is discernable that these alloys usually contain the transition metals, such as Co, Cr, Cu, Fe, Ni, to form a high-entropy base plus a relatively small amount of other transition metals, such as Al, Nb, Mo and Ti, as the eutectic forming element (EFE) to turn the single solid-solution phase to an eutectic or near-eutectic microstructure. As seen in Table 5, these EFEs do form eutectic binaries with some of the high-entropy base elements (HEBEs) or, in some cases (such as Nb), with all of the HEBEs considered.

Based on the data in Table 5, one can then follow the aforementioned formula to design the EHEAs. Here, it is worth noting that Al and Fe can form an Al-rich eutectic binary $FeAl_{2.13}$ (in atomic percentage). However, because of the large demand of Al, we consider this Al-rich eutectic binary less influential as compared to other eutectic binaries for the formation of EHEAs. As listed in Table 4, it is evident that, by excluding $FeAl_{2.13}$, the theoretically designed EHEA compositions generally agree with the experimentally determined ones, thereby supportive of the second hypothesis. Here, the legitimate question is that, if we keep increasing the amount

Table 4 Compositions of the reported EHEAs in comparison with the theoretical predictions

Reported alloys	Constituent elements	Formula	Theoretical prediction
$AlCoCrFeNi_{2.1}$ [20]	EFE: Al HEBEs: Co Cr Fe Ni	$(CoAl_{0.24})+2.1(NiAl_{0.33})$	$Al_{0.93}CoCrFeNi_{2.1}$
$Al_{1.2}CrCuFeNi_2$ [21]	EFE: Al HEBEs: Cr Cu Fe Ni	$(CuAl_{0.22})+2(NiAl_{0.33})$	$Al_{0.88}CrCuFeNi_2$
$Co_2Mo_{0.8}Ni_2VW_{0.8}$ [22]	EFE: Mo HEBEs: Co Ni Others: V W	$2(CoMo_{0.37})+2(NiMo_{0.56})$	$Co_2Mo_{1.9}Ni_2VW_{0.8}$
$CoFeNi_2V_{0.5}Nb_{0.75}$ [23]	EFE: Nb HEBEs: Co Fe Ni Others: V	$(CoNb_{0.15})+(FeNb_{0.14})+2(NiNb_{0.19})$	$CoFeNi_2V_{0.5}Nb_{0.67}$
$CoCrFeNiNb_{0.65}$ [24]	EFE: Nb HEBEs: Co Cr Fe Ni	$(CoNb_{0.15})+(CrNb_{0.15})+(FeNb_{0.14})+(NiNb_{0.19})$	$CoCrFeNiNb_{0.63}$
$CoFeNiVMo_{0.6}$ [26]	EFE: Mo HEBEs: Co Fe Ni Others: V	$(CoMo_{0.37})+(NiMo_{0.56})$	$CoFeNiVMo_{0.93}$
$CoFeNi_{1.4}VMo$ [26]	EFE: Mo HEBEs: Co Fe Ni Others: V	$(CoMo_{0.37})+1.4(NiMo_{0.56})$	$CoFeNi_{1.4}VMo_{1.15}$
$Al_{0.8}CoCrCuFeNi$ [36]	EFE: Al HEBEs: Co Cr Cu Fe Ni	$(CoAl_{0.24})+(CuAl_{0.22})+(NiAl_{0.33})$	$Al_{0.79}CoCrCuFeNi$
$Ti_{1.2}Cu_{0.8}FeCoNi$ [28]	EFE: Ti HEBEs: Cu Fe Co Ni	$0.8(CuTi_{0.37})+(FeTi_{0.19})+(CoTi_{0.3})+(NiTi_{0.19})$	$Ti_{0.98}Cu_{0.8}FeCoNi$

Table 5 Required amount (mole) of Eutectic Forming Elements (EFEs) to form eutectics [39] normalized by unit mole of High Entropy Based Elements (HEBEs)[a)]

HEBEs	EFEs			
	Al	Nb	Mo	Ti
Co	0.24	0.15	0.37	0.30
Cu	0.22	~0	–	0.37
Cr	–	0.15	–	-
Fe	2.13	0.14	–	0.19
Ni	0.33	0.19	0.56	0.19

a) Note that only the eutectic binaries stable at a low temperature are considered

of Al to above 3, for example, in the $Al_xCrCuFeNi_2$ system, would the system exhibit a eutectic microstructure? To our best knowledge, this question remains unaddressed at the present time, which could be our future work. In addition to the EFEs and HEBEs, we also identify a few elements, such as V and W, which contribute neither to the random solid solution nor to the eutectic multi-phases. According to the ref. [18], these elements were added into the alloys for other purposes. For example, adding V could lead to finer grain size and change the distribution of other constituents between dendrite and interdendritic region. Furthermore, we also calculate the S_{corr}/S_{id} ratios of the EHEAs. As seen in Figure 2(c), the calculated values fall into the range between 0.7 and 0.85, being consistent with the first hypothesis.

5 Summary

In summary, it appears that the current design of EHEAs follows a simple formula that can be traced back to the existing database of eutectic binaries. Seemingly, it also follows the empirical rules that were already established for the formation of multiple phases in HEAs. At the fundamental level, the composition of a multicomponent eutectic system should be governed by the Schroeder-van Laar equation (eq. (3)), should all eutectic phases could be known. Therefore, one improved strategy to pinpoint an EHEA composition is using the simple formula, as exemplified in Table 4, for the design of an initial EHEA composition, proceeding with the physical characterization of the eutectic phases sub-

sequently detected, and refining the initial EHEA composition with the Schroeder-van Laar equation. This whole search process could be iterative and repeated for numerous times until the final EHEA composition fits into the general thermodynamics that governs the solidification of eutectic phases in a multicomponent system.

This work was supported by the City University of Hong Kong through the UGC Block Grant with the Project (Grant No. 9610366).

1 Wattis J A D. A Becker-Döring model of competitive nucleation. J Phys A-Math Gen, 1999, 32: 8755–8784
2 Sato T, Sayama Y. Completely and partially co-operative growth of eutectics. J Cryst Growth, 1974, 22: 259–271
3 Goetzinger R, Barth M, Herlach D M. Mechanism of formation of the anomalous eutectic structure in rapidly solidified Ni-Si, Co-Sb and Ni-Al-Ti alloys. Acta Mater, 1998, 46: 1647–1655
4 Zhao S, Li J F, Liu L, et al. Cellular growth of lamellar eutectics in undercooled Ag-Cu alloy. Mater Charact, 2009, 60: 519–524
5 Jordan R M, Hunt J D. The growth of lamellar eutectic structures in the Pb-Sn and Al-$CuAl_2$ systems. Metall Mater Trans B, 1971, 2: 3401–3410
6 Johnson D R, Chen X F, Oliver B F, et al. Processing and mechanical properties of *in-situ* composites from the NiAlCr and the NiAl(Cr,Mo) eutectic systems. Intermetallics, 1995, 3: 99–113
7 Bei H, George E P, Kenik E A, et al. Directional solidification and microstructures of near-eutectic Cr-Cr_3Si alloys. Acta Mater, 2003, 51: 6241–6252
8 Bei H, George E P. Microstructures and mechanical properties of a directionally solidified NiAl-Mo eutectic alloy. Acta Mater, 2005, 53: 69–77
9 Yang W, Felton L E, Messler R W. The effect of soldering process variables on the microstructure and mechanical properties of eutectic Sn-Ag/Cu solder joints. J Electron Mater, 1995, 24: 1465–1472
10 Yeh J W, Chen S K, Lin S J, et al. Nanostructured high-entropy alloys with multiple principal elements: Novel alloy design concepts and outcomes. Adv Eng Mater, 2004, 6: 299–303
11 Ma S G, Zhang S F, Qiao J W, et al. Superior high tensile elongation of a single-crystal CoCrFeNi$Al_{0.3}$ high-entropy alloy by Bridgman solidification. Intermetallics, 2014, 54: 104–109
12 Shun T T, Du Y C. Microstructure and tensile behaviors of FCC $Al_{0.3}$CoCrFeNi high entropy alloy. J Alloy Compd, 2009, 479: 157–160
13 Senkov O N, Senkova S V, Woodward C. Effect of aluminum on the microstructure and properties of two refractory high-entropy alloys. Acta Mater, 2014, 68: 214–228
14 Senkov O N, Woodward C, Miracle D B. Microstructure and properties of aluminum-containing refractory high-entropy alloys. Jom-Us, 2014, 66: 2030–2042
15 Stepanov N D, Shaysultanov D G, Salishchev G A, et al. Effect of V content on microstructure and mechanical properties of the CoCrFeMnNiV_x high entropy alloys. J Alloy Compd, 2015, 628: 170–185
16 Hsu C Y, Wang W R, Tang W Y, et al. Microstructure and mechanical properties of new $AlCo_xCrFeMo_{0.5}$ Ni high-entropy alloys. Adv Eng Mater, 2010, 12: 44–49
17 Otto F, Dlouhý A, Somsen C, et al. The influences of temperature and microstructure on the tensile properties of a CoCrFeMnNi high-entropy alloy. Acta Mater, 2013, 61: 5743–5755
18 Senkov O N, Wilks G B, Miracle D B, et al. Refractory high-entropy alloys. Intermetallics, 2010, 18: 1758–1765
19 Wang F, Zhang Y, Chen G, et al. Tensile and compressive mechanical behavior of a CoCrCuFeNi$Al_{0.5}$ high entropy alloy. Int J Mod Phys B, 2009, 23: 1254–1259
20 Lu Y, Dong Y, Guo S, et al. A promising new class of high-temperature alloys: eutectic high-entropy alloys. Sci Rep, 2015, 4: 6200
21 Guo S, Ng C, Liu C T. Anomalous solidification microstructures in Co-free Al_xCrCuFeNi_2 high-entropy alloys. J Alloy Compd, 2013, 557: 77–81
22 Jiang H, Zhang H, Huang T, et al. Microstructures and mechanical properties of $Co_2Mo_xNi_2VW_x$ eutectic high entropy alloys. Mater Des, 2016, 109: 539–546
23 Jiang L, Lu Y, Dong Y, et al. Effects of Nb addition on structural evolution and properties of the CoFe$Ni_2V_{0.5}$ high-entropy alloy. Appl Phys A, 2015, 119: 291–297
24 He F, Wang Z, Cheng P, et al. Designing eutectic high entropy alloys of CoCrFeNiNb_x. J Alloy Compd, 2016, 656: 284–289
25 Lu Y, Gao X, Jiang L, et al. Directly cast bulk eutectic and near-eutectic high entropy alloys with balanced strength and ductility in a wide temperature range. Acta Mater, 2017, 124: 143–150
26 Jiang L, Cao Z Q, Jie J C, et al. Effect of Mo and Ni elements on microstructure evolution and mechanical properties of the CoFeNi_xVMoy high entropy alloys. J Alloy Compd, 2015, 649: 585–590
27 Zhu J M, Fu H M, Zhang H F, et al. Microstructures and compressive properties of multicomponent AlCoCrFeNiMo_x alloys. Mater Sci Eng-A, 2010, 527: 6975–6979
28 Mishra A K, Samal S, Biswas K. Solidification behaviour of Ti-Cu-Fe-Co-Ni high entropy alloys. Trans Ind Inst Met, 2012, 65: 725–730
29 He F, Wang Z, Shang X, et al. Stability of lamellar structures in CoCrFeNiNb_x eutectic high entropy alloys at elevated temperatures. Mater Des, 2016, 104: 259–264
30 Guo S, Ng C, Liu C T. Sunflower-like solidification microstructure in a near-eutectic high-entropy alloy. Mater Res Lett, 2013, 1: 228–232
31 Tsai K Y, Tsai M H, Yeh J W. Sluggish diffusion in Co-Cr-Fe-Mn-Ni high-entropy alloys. Acta Mater, 2013, 61: 4887–4897
32 Wani I S, Bhattacharjee T, Sheikh S, et al. Ultrafine-grained AlCoCrFe$Ni_{2.1}$ eutectic high-entropy alloy. Mater Res Lett, 2016, 4: 174–179
33 Dong Y, Lu Y, Kong J, et al. Microstructure and mechanical properties of multi-component AlCrFeNiMo_x high-entropy alloys. J Alloy Compd, 2013, 573: 96–101
34 Boyer H E, Gall T L. Metals Handbook Desk Edition. Metals Park: American Society for Metals, 1985
35 Ma S G, Zhang Y. Effect of Nb addition on the microstructure and properties of AlCoCrFeNi high-entropy alloy. Mater Sci Eng-A, 2012, 532: 480–486
36 Tong C J, Chen Y L, Yeh J W, et al. Microstructure characterization of Al_xCoCrCuFeNi high-entropy alloy system with multiprincipal elements. Metall Mat Trans A, 2005, 36: 881–893
37 Ivashenko A V, Titov V V, Kovshev E I. Liquid crystalline compounds: III on applicability of Schröder-Van Laar equations to liquid crystals mixtures. Mol Crysts Liquid Crysts, 1976, 33: 195–200
38 Lee H-G. Chemical Thermodynamics for Metals and Materials. Place Published: Imperial College Press,1999
39 Petzow G, Effenberg G. Ternary alloys. A comprehensive compendium of evaluated constitutional data and phase diagrams. 1991, 4
40 Dinsdale A T. SGTE data for pure elements. Calphad, 1991, 15: 317–425
41 Ternary Phase Diagrams for Materials Science. Place Published: Elsevier Science & Technology, 2001
42 Ye Y F, Wang Q, Lu J, et al. High-entropy alloy: Challenges and prospects. Mater Today, 2016, 19: 349–362
43 He Q F, Ye Y F, Yang Y. The configurational entropy of mixing of metastable random solid solution in complex multicomponent alloys. J Appl Phys, 2016, 120: 154902
44 Wang D, Tan H, Li Y. Multiple maxima of GFA in three adjacent eutectics in Zr-Cu-Al alloy system—A metallographic way to pinpoint the best glass forming alloys. Acta Mater, 2005, 53: 2969–2979
45 Ding S, Liu Y, Li Y, et al. Combinatorial development of bulk metallic

glasses. Nat Mater, 2014, 13: 494–500
46 Yeh J W. Alloy design strategies and future trends in high-entropy alloys. JOM, 2013, 65: 1759–1771
47 Ye Y F, Liu X D, Wang S, et al. The general effect of atomic size misfit on glass formation in conventional and high-entropy alloys. Intermetallics, 2016, 78: 30–41
48 Takeuchi A, Amiya K, Wada T, et al. Entropies in alloy design for high-entropy and bulk glassy alloys. Entropy, 2013, 15: 3810–3821
49 Ye Y F, Wang Q, Lu J, et al. The generalized thermodynamic rule for phase selection in multicomponent alloys. Intermetallics, 2015, 59: 75–80
50 Guo S, Liu C T. Phase stability in high entropy alloys: Formation of solid-solution phase or amorphous phase. Prog Nat Sci-Mater Int, 2011, 21: 433–446
51 Zhang Y, Lu Z P, Ma S G, et al. Guidelines in predicting phase formation of high-entropy alloys. MRC, 2014, 4: 57–62
52 Yang X, Zhang Y. Prediction of high-entropy stabilized solid-solution in multi-component alloys. Mater Chem Phys, 2012, 132: 233–238
53 Zhang Y, Peng W. Microstructural control and properties optimization of high-entrop alloys. Procedia Eng, 2012, 27: 1169–1178
54 Zhang Y, Zuo T T, Tang Z, et al. Microstructures and properties of high-entropy alloys. Prog Mater Sci, 2014, 61: 1–93
55 Mansoori G A, Carnahan N F, Starling K E, et al. Equilibrium thermodynamic properties of the mixture of hard spheres. J Chem Phys, 1971, 54: 1523–1525
56 Ye Y F, Liu C T, Yang Y. A geometric model for intrinsic residual strain and phase stability in high entropy alloys. Acta Mater, 2015, 94: 152–161
57 Zhang Y, Zhou Y J, Lin J P, et al. Solid-solution phase formation rules for multi-component alloys. Adv Eng Mater, 2008, 10: 534–538
58 Troparevsky M C, Morris J R, Kent P R C, et al. Criteria for predicting the formation of single-phase high-entropy alloys. Phys Rev X, 2015, 5: 011041
59 Highmore R J, Greer A L. Eutectics and the formation of amorphous alloys. Nature, 1989, 339: 363–365
60 Turnbull D. Under what conditions can a glass be formed? Contemp Phys, 1969, 10: 473–488